Journal of Thermal Analysis and Calorimetry (2021) 145:201–209
https://doi.org/10.1007/s10973-020-09696-7

The influence of turbulator on heat transfer and exergy drop of nanofluid in heat exchangers

Tran Dinh Manh[1] · M. Marashi[2] · Amir Mehdi Mofrad[3] · Ali Hosseini Taleghani[3] · Houman Babazadeh[4,5]

Received: 4 December 2019 / Accepted: 10 April 2020 / Published online: 27 April 2020

Abstract

In current investigation, tape is used to augment pressure drop and heat rate inside heat exchangers in existence of nanofluid. To do this, the three-dimensional model of the twisted tape is chosen for our investigation. This study dedicated on the heat transfer intensifications when significant parameters such as pitching ratio, height ratio and inlet velocity are changed. In order to simulate this model, computational fluid dynamic method with the simple algorithm is applied with k–ε (RNG) model for the modeling of the non-laminar flow through the tube due to the presence of the turbulator. Obtained results show a reasonable agreement with experimental data. Our results show that the efficiency of the H_2O-CuO nanofluid considerably increases as the Reynolds number augmented in the tube. Moreover, the rate of exergy declines (more than 35%) as the height ratio increased from 0.3 to 0.5.

Keywords Nanofluid · Turbulator · Pressure drop · Heat transfer · Heat exchanger · Turbulent flow

Introduction

Heat exchangers were the key element in the different sciences such as food production, power plant, petrochemical and textile industries. In addition, in the driers and cooling systems, heat exchangers are widely applied [1–3]. In the air conditioners, heat exchangers also used to transfer heat from the main chamber [4–6]. Since this device is highly popular and essential in the industries, engineers and researcher have tried to find the efficient model of the heat exchanger according to the applications and limitations [7–9]. Indeed, heat transfer is significant process in which the efficiency of this process could highly advance the performance of the overall systems in power plant and petrochemical industries [10–13].

There are various types of heat exchangers in the industries. The main mechanism of the heat exchanger approximately similar in all types while applied techniques for the specific purpose varies in different types of heat exchangers [6, 14–16]. In fact, the limitations of applications, operating conditions and efficiency are the main factors that highly significant in the design of each category of the heat exchangers [17–21]. Meanwhile, the type of fluid play a significant role in the type of heat exchangers [10, 21–27]. Since the performance of heat exchanger highly associated with the base fluid in the heat exchangers, various types of base fluid are examined to improve the efficiency of heat exchangers [28–30]. Indeed, the heat capacity, thermal conductivity and natural heat convection are the main characteristics of the base fluid that highly effective in the performance of the heat exchangers [29–32].

In the last decade, the use of the tiny particles (in size of nano) within the pure fluid for example water shows significant results in the heat transfer efficiency [33–35]. In fact, the existence of Ferro particles such as Al2O3 and Fe2O3 significantly changes the heat performance and characteristics of the base fluid which also alters the performance of the heat exchangers [36]. This technique varies the thermal

✉ Houman Babazadeh
houman.babazadeh@tdtu.edu.vn

1 Institute of Research and Development, Duy Tan University, Da Nang 550000, Vietnam

2 Department of Mechanical Engineering, Babol Noshirvani University of Technology, Babol, Iran

3 Department of Biomedical, Biological, and Chemical Engineering, University of Missouri, Columbia, MO, USA

4 Department for Management of Science and Technology Development, Ton Duc Thang University, Ho Chi Minh City, Vietnam

5 Faculty of Environment and Labour Safety, Ton Duc Thang University, Ho Chi Minh City, Vietnam

feature of the base fluid and it is known as nanofluid [37, 38]. Due to its effective performance, high amount of research has applied this method for developing the heat transfer rate in the various applications [39]. Indeed, the research studies in this category is extraordinary since it could offer new performance in the current heat exchangers. Hence, numerous computational packages and software are develop for this purpose. Since the flow is not complex, the commercial software offer valuable information in this topic. The review of these paper requires a significant data collection since the published papers are extraordinary growing. The readers could follow the review papers for the study of this type of heat exchangers.

Scholars and researchers have also tried to modify the heat exchanger by the thermal characteristics of the nanofluid. There are two popular technique for increasing and developing the thermal performance of heat exchangers: Active and passive systems. Sheikholeslami et al. [40] applied innovative turbulator to augment the heat rate of nanoparticles in the heat exchangers and condensers. They considered entropy generation in their simulations. They also developed numerical approach for estimation of the heat transfer in the compound turbulator [41]. They used irreversibility analysis for their investigations. The effect of hydrothermal characteristics and second law on the thermal performance of the nanofluid inside the tube is also studied by Shafee et al. [42]. They also disclose the impact of innovative turbulators on the exergy loss inside a pipe [43].

Twisted tape is recognized as an effective way for the increasing of the heat transfer in diverse models [44, 45]. Several researches [46–48] have been conducted to probe the influence of the method on the various types of heat exchangers and/or condensers such as tubular heat exchangers. They applied both computational and analytical approaches for the simulations of the heat transmission in different models. They findings is significant and reveal new aspects of the heat transfer in the nanofluid. In these researches, inclusive parametric investigations are done [4, 11, 42] to conceal the chief operative terms in the nanofluid flow. Although considerable researches have been performed in this topic, the impact of nanofluid exergy drop in the turbulator was not studies yet. It is also significant to observe all aspects of magnetic field in different sections of the heat exchangers with a turbulator. Since the cost of the computational technique is less than experimental one, numerical approach is conventionally used for the calculation of each modification in the heat exchangers.

In this research, CFD technique was employed to examine the effect of the turbulator on the thermal performance of the nanofluid through the tube. Current article tries to visualize and disclose the flow style and temperature spreading to reveal the main significant changes due to presence of the tabulator inside the tube. Our focus is mainly on the nanofluid exergy drop inside the turbulator. Besides, complete parametric evaluations are prepared to determine the power of the primary factors on the thermal performance of the nanofluid.

Computational modeling

Governing equation

To simulate the nanofluid inside the tube with turbulator, the main governing equation of the system should be initially determined. In fact, the initial step for any simulations is to define the main terms in the governing equations. Then, the reasonable computational model is chosen according to the main assumptions and boundary conditions of the real geometry of the problem. It is worthy to note that the incidence of the turbulator change the main regime of the flow inside the tube and turbulence condition should be considered in our simulations.

Following equations are the main governing equations that are used for the modeling and simulation of the flow in our problem.

$$\frac{\partial}{\partial x_{\mathrm{i}}}\left(\rho_{\mathrm{nf}} T u_{\mathrm{i}}\right) = \frac{\partial}{\partial x_i}\left(\left(\mu_{\mathrm{nf}} / \underset{\mathrm{nf}}{\mathrm{Pr}} + \mu_{\mathrm{t}} / \underset{\mathrm{t}}{\mathrm{Pr}}\right)\frac{\partial T}{\partial x_{\mathrm{i}}}\right), \tag{1}$$

$$\frac{\partial}{\partial x_{\mathrm{j}}}\left(-\overline{u_{\mathrm{i}}' u_{\mathrm{j}}'}\rho_{\mathrm{nf}}\right) - \frac{\partial p}{\partial x_{\mathrm{i}}} + \frac{\partial}{\partial x_{\mathrm{j}}}\left(\left(\frac{\partial u_{\mathrm{i}}}{\partial x_{\mathrm{j}}} + \frac{\partial u_{\mathrm{j}}}{\partial x_{\mathrm{i}}}\right)\mu_{\mathrm{nf}}\right) = \frac{\partial}{\partial x_{\mathrm{j}}}\left(u_{\mathrm{i}} u_{\mathrm{j}} \rho_{\mathrm{nf}}\right) \tag{2}$$

$$\frac{\partial}{\partial x_{\mathrm{i}}}\left(u_{\mathrm{i}}\right) = 0 \tag{3}$$

$\rho_{\mathrm{nf}}\overline{u_{\mathrm{j}}' u_{\mathrm{i}}'}$ and μ_{t} are:

$$-\overline{u_{\mathrm{j}}' u_{\mathrm{i}}'}\rho_{\mathrm{nf}} = \mu_{\mathrm{t}}\left(\frac{\partial u_{\mathrm{i}}}{\partial x_{\mathrm{j}}} + \frac{\partial u_{\mathrm{j}}}{\partial x_{\mathrm{i}}}\right) - \frac{2}{3}\rho_{\mathrm{nf}} k \delta_{\mathrm{ij}} - \frac{2}{3}\mu_{\mathrm{t}}\frac{\partial u_{\mathrm{k}}}{\partial x_{\mathrm{k}}}\delta_{\mathrm{ij}} \tag{4}$$

$$\mu_{\mathrm{t}} = \rho_{\mathrm{nf}} C_{\mu} k^2 / \varepsilon \tag{5}$$

k, ε could be determined via:

$$\begin{gathered}\frac{\partial}{\partial x_{\mathrm{j}}}\left(\left(\frac{\mu_{\mathrm{t}}}{\sigma_{\mathrm{k}}} + \mu_{\mathrm{nf}}\right)\frac{\partial k}{\partial x_{\mathrm{j}}}\right) - \rho_{\mathrm{nf}}\varepsilon + G_{\mathrm{k}} = \frac{\partial}{\partial x_{\mathrm{i}}}\left(u_{\mathrm{i}}\rho_{\mathrm{nf}} k\right), \\ G_{\mathrm{k}} = -\frac{\partial u_{\mathrm{j}}}{\partial x_{\mathrm{i}}}\rho_{\mathrm{nf}}\overline{u_{\mathrm{j}}' u_{\mathrm{i}}'}\end{gathered} \tag{6}$$

$$\frac{\partial}{\partial x_{\mathrm{i}}}\left(u_{\mathrm{i}}\rho_{\mathrm{nf}}\varepsilon\right) = \frac{\partial}{\partial x_{\mathrm{j}}}\left(\left(\frac{\mu_{\mathrm{t}}}{\sigma_{\varepsilon}} + \mu_{\mathrm{nf}}\right)\frac{\partial \varepsilon}{\partial x_{\mathrm{j}}}\right) + \frac{\varepsilon}{k}G_{\mathrm{k}}C_{1\varepsilon} - \rho_{\mathrm{nf}}\frac{\varepsilon^2}{k}C_{2\varepsilon} \tag{7}$$

$$C_{1\varepsilon} = 1.42,\ C_{\mu} = 0.0845,\ C_{2\varepsilon} = 1.68, \Pr_{t} = 0.85, \sigma_{k} = 1, \sigma_{\varepsilon} = 1.3 \tag{8}$$

Since the main significant terms of the nanofluid is associated to the hydrothermal characteristic of the nanoparticles within the main fluid, we modified heat conductivity, heat capacity and density of the fluid according to the nanofluid characteristics. Hence,$\left(\rho C_{p}\right)_{nf}$, ρ_{nf}, k_{nf} and μ_{nf} are calculated as follows:

$$\left(\rho C_{p}\right)_{nf} = \left(\rho C_{p}\right)_{f}(1-\phi) + \left(\rho C_{p}\right)_{s}\phi \tag{9}$$

$$\rho_{nf} = \rho_{f}(1-\phi) + \rho_{s}\phi \tag{10}$$

Grid generation and Boundary conditions

In this step, the grid should be generated for the computational method. As shown in the Fig. 1, unstructured grid is produces due the presence of the turbulator. In previous studies, full details of the applied grid are presented.

After determining the main governing equation and production of grid, the applied boundary condition of the problem should be defined. Figure 1 illustrates the model with the main size. As shown in the figure, the turbulator is presented in the middle of the tube and the nanofluid is entered from the left side. Therefore, we applied following boundary conditions for our model:

$$\begin{aligned}
\frac{k_{nf}}{k_{f}} &= 1 + 3\frac{\phi\left(-1 + k_{p}/k_{f}\right)}{\phi\left(1 - k_{p}/k_{f}\right) + \left(2 + k_{p}/k_{f}\right)} + 5\times 10^{4} g'(\phi, T, d_{p})\phi\rho_{f}c_{p,f}\sqrt{\frac{\kappa_{b}T}{\rho_{p}d_{p}}} \\
g'\left(\phi, T, d_{p}\right) &= \left(a_{1} + a_{2}Ln\left(d_{p}\right) + a_{5}Ln\left(d_{p}\right)^{2} + a_{3}Ln(\phi) + a_{4}Ln(\phi)\ln\left(d_{p}\right)\right)Ln(T) \\
&+ \left(a_{6} + a_{7}Ln\left(d_{p}\right) + a_{10}Ln\left(d_{p}\right)^{2} + a_{8}Ln(\phi) + a_{9}\ln\left(d_{p}\right)Ln(\phi)\right),
\end{aligned} \tag{11}$$

$$\frac{\mu_{nf}}{\mu_{f}} = \frac{1}{(1-\phi)^{2.5}} + \frac{k_{Brownian}}{\Pr\ k_{f}} \tag{12}$$

$$v_{i} = 0, u_{i} = 0, T_{i} = cte, w_{i} = cte, I = (\mathrm{Re})^{\frac{-1}{8}}0.16 \tag{13}$$

$$\frac{\partial v}{\partial z} = \frac{\partial u}{\partial z} = \frac{\partial w}{\partial z} = 0, \frac{\partial T}{\partial z} = 0 \tag{14}$$

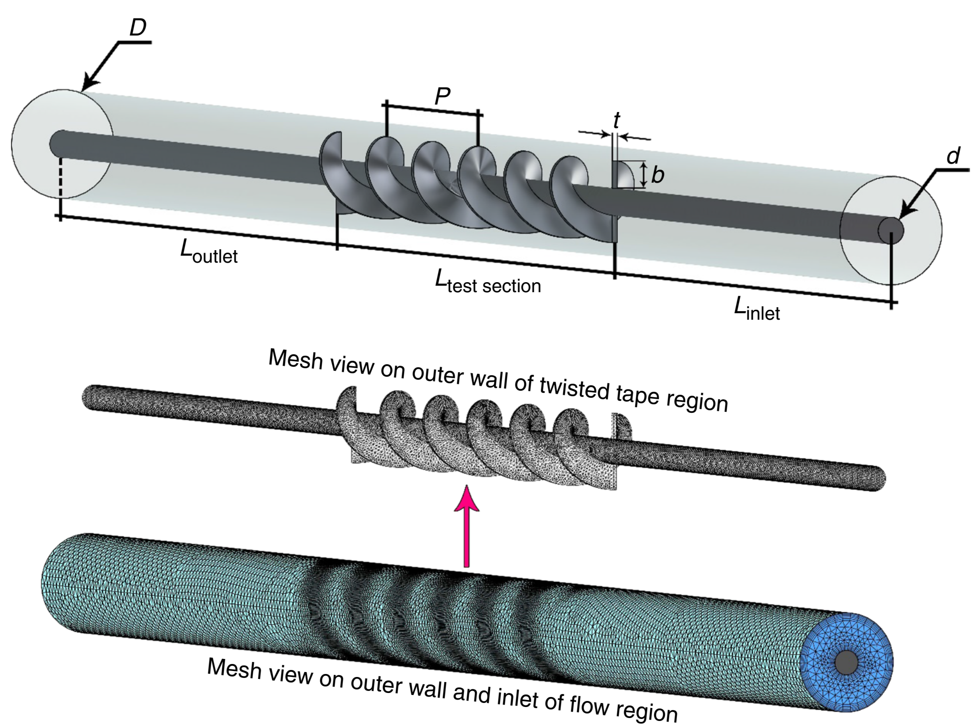

Fig. 1 Nanomaterial inside a tube with turbulator

Non-dimensional heat transfer is known as Nusselt number (Nu), and f is pressure drop in the following equation:

$$\mathrm{Nu} = \frac{hD_h}{k}, \quad f = \frac{\Delta p}{\frac{\rho v_m^2}{2}\frac{L}{D_h}}, X_d = T_0 S_{\text{gen,total}} \tag{15}$$

.

Computational technique

In order to simulate the nanofluid inside the tube with tabulator, ANSYS software is applied as robust software to simulate this problem. The simple algorithm is chosen as a reliable numerical scheme for the simulation of incompressible flow inside the tube. In addition, k-ε (RNG) type is selected for the calculation of turbulent viscosity since the flow with nanoparticles is turbulent in our investigation. In Ref. [42] summarizes the information of simulation set up.

Results and discussion

In order to assess the acquired results, validation is the first step to ensure the method and approaches. Figure 2 illustrates the heat transfer rate in terms of *h(x)* for different x/D. In this figure, the results of our simulations are associated with experimental results of Kim et al. [43]. Obtained results clearly confirm the precision of the obtained data and the numerical discrepancy is less than 12% in different models.

Figure 3a depicted the contour of temperature, velocity and X_d in the three sections of $Z=0.3$, 0.45 and 0.6 for PR = 15, BR = 0.3, Re = 5000. In addition, the streamline of these cross sections also presented. The gained fallouts clearly show that the temperature decreases along the turbolator. The results of the streamline visibly confirm that the flow becomes turbulent as nanofluid moves along the turbulator. Figure 3b illustrates contour of temperature, velocity and exergy (X_d) in PR = 15, BR = 0.3, Re = 20,000. In this figure, the velocity of the nanofluid significantly increases and this considerably enhances the turbulence in the model. The results of exergy change also approve the high heat transfer in the vicinity of the tube wall. In high Reynolds number, the variation of the exergy increases along the tube. As shown in the figure, the high exergy region is limited in the entrance of the tube and the exergy rate augments in the vicinity of the tube wall at $z=0.6$.

To recognize the main effect of turbulator, the effect of height ratio on the flow and temperature distribution is demonstrated in the Fig. 4a. In this model the size of the height ratio is increased from 0.3 to 0.5. The initial effect of this change is visible in the temperature penetration inside the model. Meanwhile, the intensity of the flow circulation highly increases along the turbulator. Figure 4b illustrates the influence of the inlet velocity in the flow pattern and temperature distribution of the model when Reynolds number is 20,000. The results of the exergy (X_d) is significant in the high inlet velocity. As depicted in the figure, the variation of the exergy in the tip of the turbulator blade is higher than other sections. In addition, the high exergy region also occurs in the vicinity of the tube which is close to the blade of the turbulator.

Figure 5 demonstrates the impact of pitch ratio reduction on the flow structure and temperature distributions in different sections along the turbulator. As shown in the Fig. 5a, the streamline becomes more uniform as the pitch ratio declines to 5. In the high Reynolds number (Re = 20,000), the streamline change decreases along the tube.

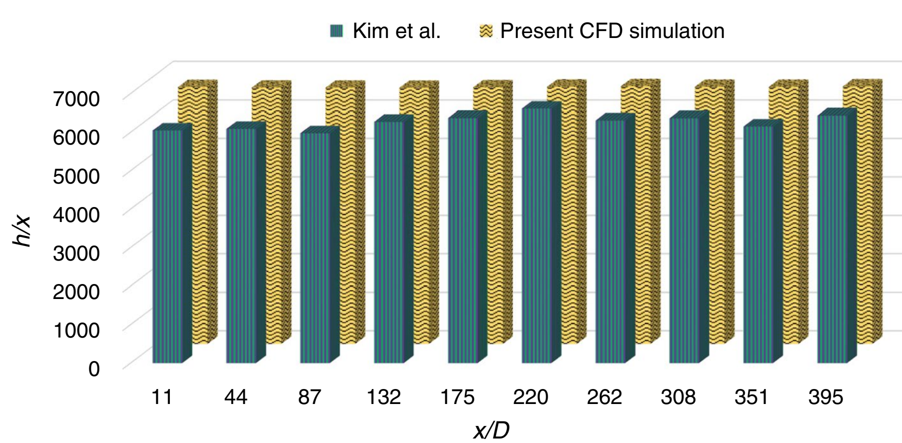

Fig. 2 Verification with older paper [43]

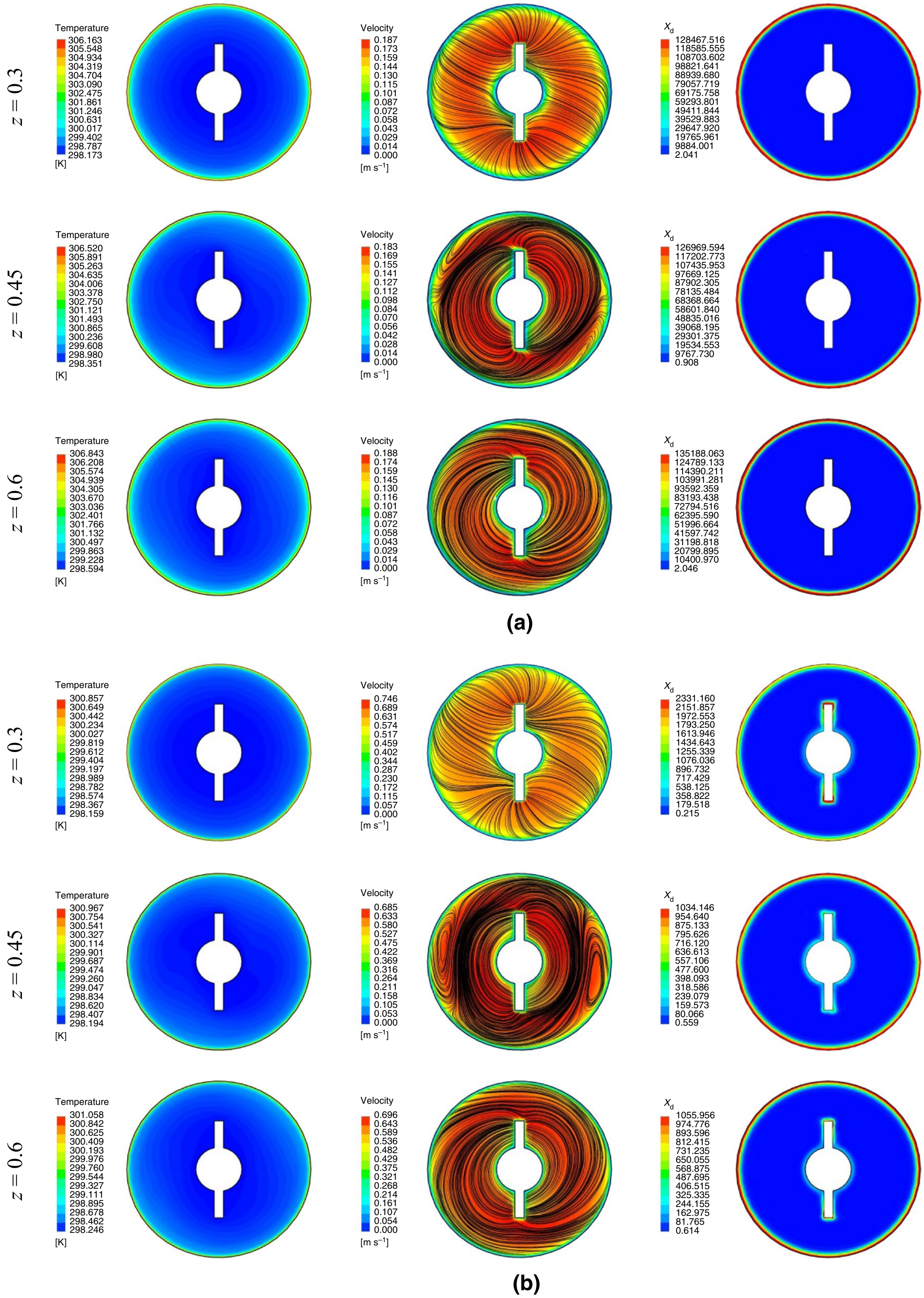

Fig. 3 Contours of T, X_d, and velocity for **b** Re = 20,000, **a** Re = 5000 when BR = 0.3, PR = 15

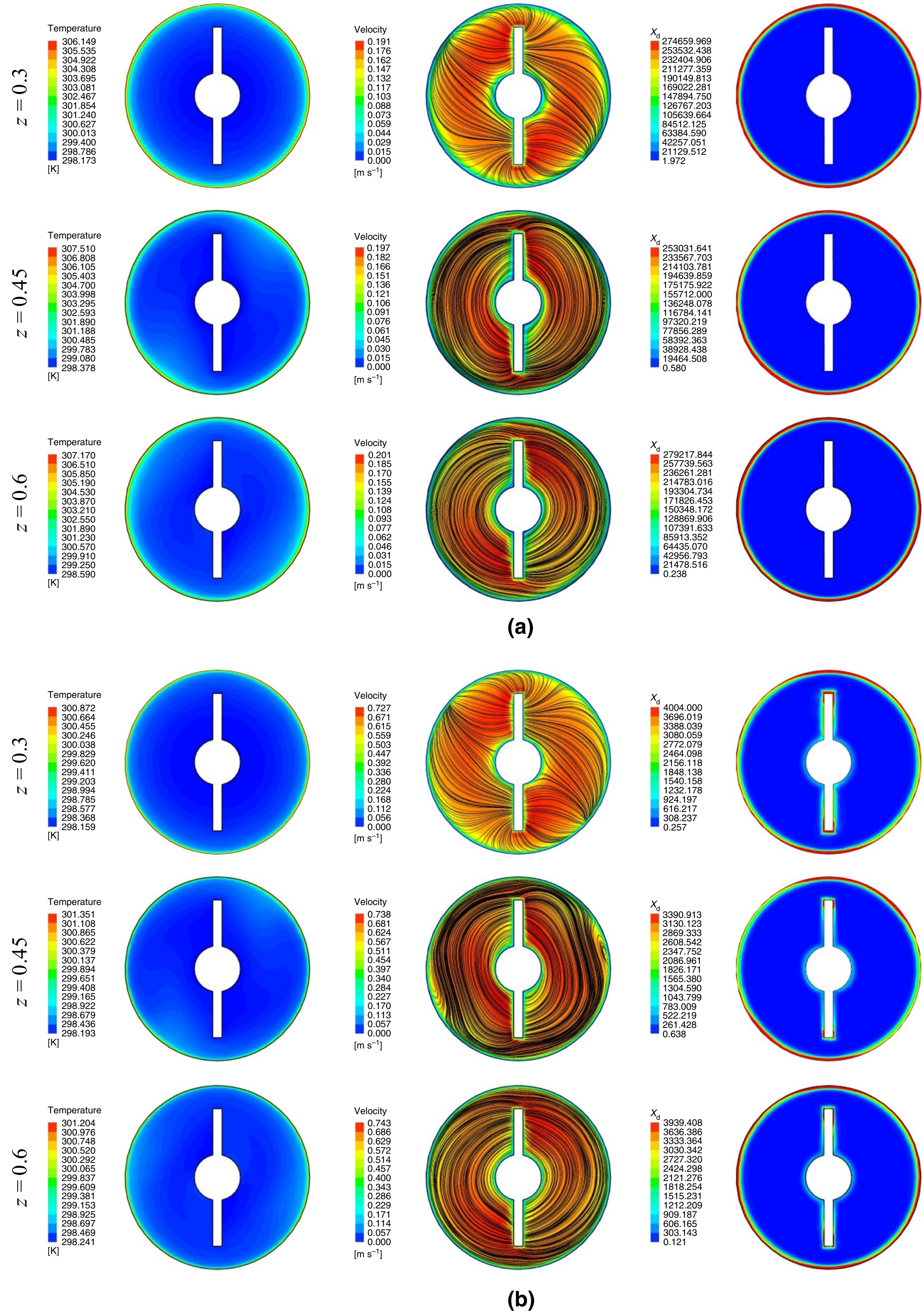

Fig. 4 Contours of T, X_d, and velocity for **b** Re = 20,000, **a** Re = 5000 when BR = 0.5, PR = 15

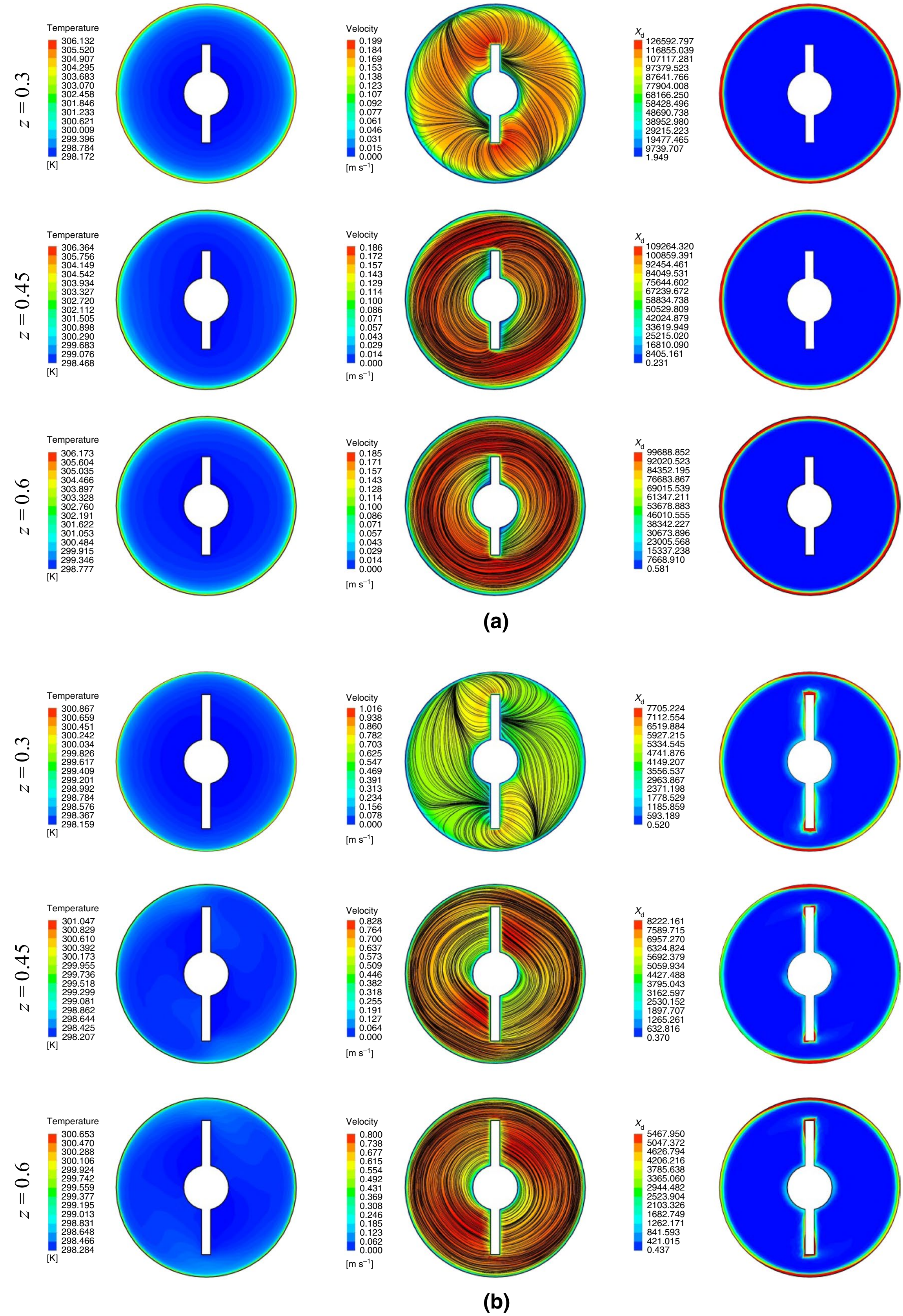

Fig. 5 Contours of T, X_d, and velocity for **a** Re = 5000 **b** Re = 20,000 when PR = 5, BR = 0.3

Conclusion

In this study, the effects of turbulator the thermal efficiency of heat exchanger with nanofluid is simulated Computational fluid Dynamic (CFD). The key aim of this article is to examine the impact of significant factors such as pitch ratio (= 15, 5), height ratio and inlet velocity on the hydrothermal characteristics of H_2O-CuO nanofluid in our model. The contours of temperature, velocity as well as streamline and exergy (X_d) are compared in the several distinctive operating conditions. Our findings evidently display that the turbulator strengthens the heat efficincy and this intensifies by the increasing of the inlet velocity.

References

1. Manh TD, Bahramkhoo M, Gerdroodbary MB, Nam ND, Tlili I. Investigation of nanomaterial flow through non-parallel plates. J Therm Anal Calorim. 2020. https://doi.org/10.1007/s10973-020-09352-0.
2. Wang P, Li JB, Bai FW, Liu DY, Xu C, Zhao L, Wang ZF. Experimental and theoretical evaluation on the thermal performance of a windowed volumetric solar receiver. Energy. 2017;119(15):652–61.
3. Qin Y, Zhang M, Hiller JE. Theoretical and experimental studies on the daily accumulative heat gain from cool roofs. Energy. 2017;129:138–47.
4. Sheikholeslami M, Gerdroodbary M, Shafee A, Tlili I. Hybrid nanoparticles dispersion into water inside a porous wavy tank involving magnetic force. J Therm Anal Calorim. 2019. https://doi.org/10.1007/s10973-019-08858-6.
5. Mihaiu S, Szilágyi IM, Atkinson I, Mocioiu OC, Hunyadi D, Pandele-Cusu J, Toader A, Munteanu C, Boyadjiev S, Madarász J, Pokol G, Zaharescu M. Thermal study on the synthesis of the doped ZnO to be used in TCO films. J Therm Anal Calorim. 2016;124(1):71–80.
6. Manh TD, Nam ND, Abdulrahman GK, Moradi R, Babazadeh H. The influence of Hybrid nanoparticles transportation on natural convection inside porous domain. Int J Mod Phys C. 2020;31(02):2050026.
7. Cao L, Chaoyu T, Pengfei H, Liu S. Influence of solid particle erosion (SPE) on safety and economy of steam turbines. Appl Therm Eng. 2019;150(5):552–63.
8. Gao W, Wang WF. The eccentric connectivity polynomial of two classes of nanotubes. Chaos Solitons Fractals. 2016;89:290–4.
9. Shafee A, Firouzi A, Nam ND, Babazadeh H. Elliptic cavity filled with hybrid nanomaterial under consideration of magnetic field. Int J Mod Phys C. 2020. https://doi.org/10.1142/S0129183120500801.
10. Qin Y, Zhang M, Mei G. A new simplified method for measuring the permeability characteristics of highly porous media. J Hydrol. 2018;562:725–32.
11. Tang G, Shafee A, Nam ND, Tlili I. Coulomb forces impacts on nanomaterial transportation within porous tank with lid walls. J Therm Anal Calorim. 2020. https://doi.org/10.1007/s10973-020-09407-2.
12. Qin Y, Zhao Y, Chen X, Wang L, Li F, Bao T. Moist curing increases the solar reflectance of concrete. Constr Build Mater. 2019;215:114–8.
13. Sheikholeslami M, Jafaryar M, Shafee A, Babazadeh H. Acceleration of discharge process of clean energy storage unit with insertion of porous foam considering nanoparticle enhanced paraffin. J Clean Prod. 2020;261:121206. https://doi.org/10.1016/j.jclepro.2020.121206.
14. Gao W, Yan L, Shi L. Generalized Zagreb index of polyomino chains and nanotubes. Optoelectron Adv Mater Rapid Commun. 2017;11(1–2):119–24.
15. Zhang Y, Zhang X, Li M, Liu Z. Research on heat transfer enhancement and flow characteristic of heat exchange surface in cosine style runner. Heat Mass Transf. 2019;55:3117–31.
16. Babazadeh H, Ambreen T, Shehzad SA, Shafee A. Ferrofluid non-Darcy heat transfer involving second law analysis; An application of CVFEM. J Therm Anal Calorim. 2020. https://doi.org/10.1007/s10973-020-09264-z.
17. Qin Y, He Y, Hiller JE, Mei G. A new water-retaining paver block for reducing runoff and cooling pavement. J Clean Prod. 2018;199:948–56.
18. Fu G, Guo J, Yao X, Summers PA, Widijatmoko SD, Hall P. An investigation of the current status of recycling spent lithium-ion batteries from consumer electronics in China. J Clean Prod. 2017;161(10):765–80.
19. Qin Y, Hiller JE. Understanding pavement-surface energy balance and its implications on cool pavement development. Energy Build. 2014;85:389–99.
20. Szilágyi IM, Kállay-Menyhárd A, Šulcová P, Kristóf J, Pielichowski K, Šimon P. Recent advances in thermal analysis and calorimetry presented at the 1st Journal of Thermal Analysis and Calorimetry Conference and 6th V4 (Joint Czech-Hungarian-Polish-Slovakian) Thermoanalytical Conference (2017). J Therm Anal Calorim. 2018;133:1–4.
21. Gao W, Wang WF. The vertex version of weighted wiener number for bicyclic molecular structures, Computational and Mathematical Methods in Medicine, 2015, 10, Article ID 418106. http://dx.doi.org/10.1155/2015/418106.
22. Manh TD, Salehi F, Shafee A, Nam ND, Shakeriaski F, Babazadeh H, Vakkar A, Tlili I. Role of magnetic force on the transportation of nano powders including radiation. J Therm Anal Calorim. 2019. https://doi.org/10.1007/s10973-019-09182-9.
23. Szilágyi IM, Santala E, Heikkilä M, Kemell M, Nikitin T, Khriachtchev L, Räsänen M, Ritala M, Leskelä M. Thermal study on electrospun polyvinylpyrrolidone/ammonium metatungstate nanofibers: optimising the annealing conditions for obtaining WO3 nanofibers. J Therm Anal Calorim. 2011;105(1):73.
24. Ji Q, Guo J-F. Oil price volatility and oil-related events: an Internet concern study perspective. Appl Energy. 2015;137(1):256–64.
25. Lublóy É, Kopecskó K, Balázs GL, Szilágyi IM, Madarász J. Improved fire resistance by using slag cements. J Therm Anal Calorim. 2016;125(1):271–9.
26. Seyednezhad M, Sheikholeslami M, Ali JA, Shafee A, Nguyen TK. Nanoparticles for water desalination in solar heat exchanger Review. J Therm Anal Calorim. 2020;139:1619–36. https://doi.org/10.1007/s10973-019-08634-6.
27. Gao W, Farahani MR, Shi L. The forgotten topological index of some drug structures. Acta Medica Mediterranea. 2016;32:579–85.
28. Qin Y. Urban canyon albedo and its implication on the use of reflective cool pavements. Energy Build. 2015;96:86–94.
29. Wang G, Wang F, Shen F, Jiang T, Chen Z, Peng H. Experimental and optical performances of a solar CPV device using a linear Fresnel reflector concentrator. Renew Energy. 2020;146:2351–61.
30. Qin Y. A review on the development of cool pavements to mitigate urban heat island effect. Renew Sustain Energy Rev. 2015;52:445–59.

31. Babazadeh H, Shah Z, Ullah I, Kumam P, Shafee A. Analyze of hybrid nanofluid behavior within a porous cavity including Lorentz forces and radiation impacts. J Therm Anal Calorim. 2020. https://doi.org/10.1007/s10973-020-09416-1.
32. Qin Y, Luo J, Chen Z, Mei G, Yan L-E. Measuring the albedo of limited-extent targets without the aid of known-albedo masks. Sol Energy. 2018;171:971–6.
33. Manh TD, Nam ND, Abdulrahman GK, Moradi R, Babazadeh H. Impact of MHD on hybrid nanomaterial free convective flow within a permeable region. J Therm Anal Calorim. 2019. https://doi.org/10.1007/s10973-019-09008-8.
34. Qin Y, Hiller JE, Meng D. Linearity between pavement thermophysical properties and surface temperatures. J Mater Civil Eng. 2019. https://doi.org/10.1061/(ASCE)MT.1943-5533.0002890.
35. Hajizadeh MR, Selimefendigil F, Muhammad T, Ramzan M, Babazadeh H, Li Z. Solidification of PCM with nano powders inside a heat exchanger. J Mol Liquids. 2020;306:112892.
36. Sheikholeslami M. New computational approach for exergy and entropy analysis of nanofluid under the impact of Lorentz force through a porous media. Comput Methods Appl Mech Eng. 2019;344:319–33.
37. Mofrad AM, Schellenberg Parker S, Peixoto C, Hunt Heather K, Hammond Karl D. Calculated infrared and Raman signatures of Ag^{+}, Cd^{2+}, Pb^{2+}, Hg^{2+}, Ca^{2+}, Mg^{2+}, and K^{+} sodalites. Microporous Mesoporous Mater. 2020;296:109983.
38. Qin Y, He H, Ou X, Bao T. Experimental study on darkening water-rich mud tailings for accelerating desiccation. J Clean Prod. 2019. https://doi.org/10.1016/j.jclepro.2019.118235.
39. Iasir ARM, Lombardi T, Lu Q, Mofrad AM, Vaninger M, Zhang X, Singh DJ. Electronic and magnetic properties of perovskite selenite and tellurite compounds: CoSeO 3, NiSeO 3, CoTeO 3, and NiTeO 3. Phys Rev. 2020;101(4):045107.
40. Sheikholeslami M, Gerdroodbary MB, Moradi R, Shafee A, Li Z. Application of Neural Network for estimation of heat transfer treatment of Al_2O_3-H_2O nanofluid through a channel. Comput Methods Appl Mech Eng. 2019;344(2019):1–12.
41. Dinh MT, Tlili I, Dara RN, Shafee A, Al-Jahmany YYY, Nguyen-Thoi T. Nanomaterial treatment due to imposing MHD flow considering melting surface heat transfer. Physica A Physica A. 2020;540:123036.
42. Sheikholeslami M, Jafaryar M, Shafee A, Li Z. Nanofluid heat transfer and entropy generation through a heat exchanger considering a new turbulator and CuO nanoparticles. J Therm Anal Calorim. 2019. https://doi.org/10.1007/s10973-018-7866-7.
43. Shafee A, Sheikholeslami M, Jafaryar M, Babazadeh H. Irreversibility of hybrid nanoparticles within a pipe fitted with turbulator. J Therm Anal Calorim. 2020. https://doi.org/10.1007/s10973-019-09248-8.
44. Shafee A, Jafaryar M, Abohamzeh E, Nam ND, Tlili I. Simulation of thermal behavior of hybrid nanomaterial in a tube improved with turbulator. J Therm Anal Calorim. 2020. https://doi.org/10.1007/s10973-019-09247-9.
45. Kim D, Kwon Y, Cho Y, Li C, Cheong S, Hwang Y, Lee J, Hong D, Moona S. Convective heat transfer characteristics of nanofluids under laminar and turbulent flow conditions. Curr Appl Phys. 2009;9:e119–23.
46. Mofrad AM, Peixoto C, Blumeyer J, Liu J, Hunt HK, Hammond KD. Vibrational spectroscopy of sodalite: theory and experiments. J Phys Chem C. 2018;122(43):24765–79.
47. Manh TD, Nam ND, Abdulrahman GK, Khan MH, Tlili I, Shafee A, Shamlooei M, Nguyen-Thoi T. Investigation of hybrid nanofluid migration within a porous closed domain. Phys A Stat Mech Appl. 2020. https://doi.org/10.1016/j.physa.2019.123960.
48. Dongmin Yu, Zhu H, Han W, Holburn D. Dynamic multi agent-based management and load frequency control of PV/Fuel cell/wind turbine/CHP in autonomous microgrid system. Energy. 2019;173(15):554–68.

Publisher's Note Springer Nature remains neutral with regard to jurisdictional claims in published maps and institutional affiliations.